



A numerical method for simulating discontinuous shallow flow over an infiltrating surface

* Roshni Patel ** Jitendrasinh D. Raol.

*, ** P.G .student, M.E. (Civil), WRM, Department of Civil Engineering, L.D. College of Engineering, Ahmadabad

ABSTRACT

A numerical method based on the Mac Cormack finite difference scheme was developed for simulating two-dimensional overland flow with spatially variable infiltration and micro-topography using the hydrodynamic flow equations. The Mac Cormack scheme is enhanced by using the method of fractional steps to simplify application; treating the friction slope, a stiff source term, point-implicitly, plus, for numerical oscillation control and stability, up winding the convective acceleration term. The developed method will also be useful for simulating irrigation, tidal flat and wetland circulation, and floods.

Keywords : Finite difference Shallow water equations, Mac Cormack scheme.

1. INTRODUCTION

Hydrologists are often faced with the challenge of predicting the timing and magnitude of “rainfall-generated run-off from watersheds for flood control, pollution prevention and ecological purposes. An important component of the rainfall run-off process is Horton an overland flow, which is the shallow flow of water over the land surface prior to the major channelization that results when the rainfall rate exceeds the soil infiltration capacity in at least some areas of the watershed.

This paper presents a numerical method based on the Mac Cormack finite difference scheme developed for simulating two-dimensional, spatially variable overland flow at a small scale. The equations that describe this process are very similar to the well-known St. Venant and shallow water equations, thus, the developed numerical method or aspects thereof can be applied to a wide range of shallow water flow problems where discontinuous regimes are expected, such as irrigation, tidal flat circulation, flow in ephemeral stream channels and flash floods.

2. EQUATIONS

The two-dimensional hydrodynamic overland flow equations can be derived from the Navier-Stokes equations, by averaging over depth using kinematic boundary conditions and making certain assumptions, including: that

- (a) Velocity is constant with depth,
- (b) The vertical velocity and acceleration components are small,
- (c) The pressure distribution is hydrostatic, and horizontal shear stresses are small.

In terms of the dependent variables, depth, h, and unit discharge in the x- and y-directions, qx and qy respectively, these equations are

$$\frac{\partial h}{\partial t} + \frac{\partial q_x}{\partial y} + \frac{\partial q_y}{\partial x} - q_1 = 0, \dots \dots \dots (1)$$

$$\frac{\partial q_x}{\partial t} + \frac{\partial}{\partial x} \left(\frac{q_x^2}{h} + \frac{gh^2}{2} \right) + \frac{\partial}{\partial y} \left(\frac{q_x q_y}{h} \right) - gh(S_{ox} - S_{tx}) = 0.. (2)$$

$$\frac{\partial q_y}{\partial t} + \frac{\partial}{\partial y} \left(\frac{q_y^2}{h} + \frac{gh^2}{2} \right) + \frac{\partial}{\partial x} \left(\frac{q_x q_y}{h} \right) - (ghS_{ox} - S_{ty}) = 0, (3)$$

Equation (1) results from conservatoire of-mass over a control volume, and Equations (2) and (3) result from conserva-

tion of momentum in the x- and y-directions respectively. The source term q1, lateral inflow, is the rate of water vertically added to or removed from the control volume. The various differential terms in the momentum equations represent different quantities related to conservation of momentum in the x-: direction, these terms are analogous to the terms in the classical St. Venant equations as follows.

- $\frac{\partial}{\partial x} \left(\frac{\rho h^3}{2} \right)$ Pressure force
- $\frac{\partial q_x}{\partial t}$ Local acceleration
- $\frac{\partial}{\partial x} \left(\frac{q_x^2}{h} \right), \frac{\partial}{\partial y} \left(\frac{q_x q_y}{h} \right)$ Convective acceleration

The y-direction terms are related similarly.

The bed slopes, $S_{ox} = \frac{\partial z}{\partial x}, S_{oy} = \frac{\partial z}{\partial y}$ (4)

Measured data are used to estimate these slopes in a manner that must be consistent with the numerical scheme; various methods exist for the evaluation of the friction slope terms, S_{fx} and S_{fy}. The two-dimensional form of the Darcy-Weisbach (D-W) equation is primarily used to compute the friction slopes herein

$$S_{fx} = \frac{f}{8g} \frac{q_x (q_x^2 + q_y^2)^{1/2}}{h^3}, S_{fy} = \frac{f}{8g} \frac{q_y (q_x^2 + q_y^2)^{1/2}}{h^3}, \dots \dots (5)$$

Where f is the D-W friction factor Natural overland flow is generally laminar, but is ‘disturbed’ by rainfall and topographic irregularities [4]. In the laminar flow regime, in which viscous stresses are much larger than Reynolds stresses, f is computed as a function “of Reynolds number, Re, by the equation

$$f = \frac{K_0}{Re} \dots \dots \dots (6)$$

Where Ko is a resistance parameter related to the ground surface characteristics. The Reynolds number for two-dimensional flow is computed as

$$Re = \frac{(q_x^2 + q_y^2)^{1/2}}{\nu} \dots \dots \dots (7)$$

3. NUMERICAL METHOD

Mac Cormack’s explicit predictor-corrector finite difference method was chosen as the basic scheme after a review of the various numerical methods available this scheme has been “successfully used to solve similar equations for the system of

overland flow equations in two dimensions it is written

$$U_{j,k}^n = U_{j,k}^{n-1} - \frac{\Delta t}{\Delta x} (G_{j,k}^n - G_{j-1,k}^n) - \frac{\Delta t}{\Delta x} (H_{j,k}^n - H_{j,k-1}^n) + \Delta t S_{j,k}^n \dots\dots\dots (8)$$

$$U_{j,k}^{n+1} = 0.5 \left[U_{j,k}^n + U_{j,k}^{*n} - \frac{\Delta t}{\Delta x} (G_{j+1}^* - G_{j,k}^*) - \frac{\Delta t}{\Delta x} (H_{j,k+1}^* - H_{j,k}^*) + \Delta t S_{j,k}^* \right] \dots\dots\dots (9)$$

The subscripts J and K & are spatial indices in the x- and y- directions respectively, and the superscript n refers to

the time level where v is the kinematic viscosity of water After substitution, the laminar flow friction slope terms become

$$S_{f_x} = \frac{K_o v q_y}{\theta g h^3}, S_{f_y} = \frac{K_o v q_x}{\theta g h^3} \dots\dots\dots (10)$$

To account for turbulent momentum transfer the well-known second-order turbulent viscosity terms

$$\epsilon_l \left(\frac{\partial^2}{\partial x^2} + \frac{\partial^2 q_x}{\partial y} \right), \epsilon_l \left(\frac{\partial^2}{\partial x^2} + \frac{\partial^2 q_y}{\partial y^2} \right) \dots\dots\dots (11)$$

Can be added in the x- and y directions respectively In these terms, is the coefficient of turbulent viscosity or eddy coefficient.

The overland flow equations are presented here in vector form

In these equations, T denotes the transpose; G (U) and H (U)

$$\frac{\partial U}{\partial t} + \frac{\partial G(U)}{\partial x} + \frac{\partial H(U)}{\partial y} = S(U) \dots\dots\dots (12)$$

Where $U = [j, q_x, q_y]^T \dots\dots\dots (13)$

$$G(U) = \left[q_x, \frac{q_x^2}{h} + \frac{qh^2}{2}, \frac{q_x q_y}{h} \right]^T \dots\dots\dots (14)$$

$$H(U) = \left[q_y, \frac{q_y^2}{h} + \frac{qh^2}{2}, \frac{q_x q_y}{h} \right]^T \dots\dots\dots (15)$$

$$S(U) = \left[q_l - gh \frac{\partial z}{\partial x} - \frac{K_o v q_x}{8h^2} + \epsilon_l \left(\frac{\partial^2 q_x}{\partial x^2} + \frac{\partial^2 q_y}{\partial y^2} \right) - gh \frac{\partial z}{\partial y} - \frac{K_o v q_y}{8h^2} + \left(\frac{\partial^2 q_x}{\partial x^2} + \frac{\partial^2 q_y}{\partial y^2} \right) \right]^T \dots\dots\dots (16)$$

are referred to as flux vectors, and S (U) as the source vector. Here after, these vectors will be shown as G, H and S, but the dependence on the vector of dependent variables U remains.

The dependent variable vector predicted with Equation denoted with an *, is used to compute the differences in the corrector step As shown, backward spatial differences are used in the predictor step, and forward spatial differences in the corrector. In order to obtain second-order accuracy with the Mac Cormack, scheme, It. is necessary to alternate the spatial difference sequence in time Here, for example, a forward-backward difference sequence would be used to compute U^{n+2} . This form has been used, previously for less spatially variable overland flow computations. Appropriate initial and boundary conditions must be specified. For the-desired simulation, the appropriate initial condition is zero depth and zero unit discharge everywhere in the domain. The best way to handle this initial condition is to assign small, significant starting depth the values used are discussed in subsequent paragraph in experimental plot overland flow simulations (rectangular plots), the subject of another aspect of this research for which this model was developed, closed boundaries formed by metal walls on three sides allow no through flow, so qx and

qy perpendicular to these boundaries is set to zero. Depths at closed boundaries are determined by using inward differences in the continuity equation. At the plot outlet, an open boundary is simulated by using inward differences in both the continuity and momentum equations. Other boundary conditions are easily implemented for different applications.

The maximum time step (with respect to stability) allowable in the Mac Cormack scheme applied to linear hyperbolic equations is limited by the well-known Courant-Friedrich-Lowy (CFL) condition, as are all explicit finite difference methods.

(A) Method of fractional steps

Two-dimensional finite difference schemes for systems of hyperbolic equations are sometimes split into a series of one-dimensional finite difference operators known as fractional step A fractional step Mac Cormack scheme has been previously applied to the St. Venant equations and used to simulate reservoir and river flows In addition to simplifying application of the scheme to a two-dimensional problem, those authors found that larger time steps can be used. The fractional step Mac Cormack scheme is written

$$U_{j,k}^{n+1} = L_x 2(\Delta t/2) L_y 2(\Delta t/2) L_x 1(\Delta t/2) L_y 1(\Delta t/2) U_{j,k}^n \dots\dots\dots (17)$$

Where Lx and Ly are one-dimensional difference operators, each applied twice and in a symmetrical manner. The first x-direction operator, Lxl, is written

$$U_{j,k}^* = U_{j,k}^n - \frac{\Delta t}{2\Delta x} (G_{j,k}^n - G_{j-1,k}^n) + \frac{\Delta t}{2\Delta x} S_{x1,j,k}^n \dots\dots (18)$$

$$U_{j,k}^{**} = 0.5 \left[U_{j,k}^n - U_{j,k}^* (G_{j+1,k}^* - G_{j,k}^*) + \frac{\Delta t}{2} S_{x1,j,k}^* \right] (19)$$

Only the x-direction flux vector and source terms are used to compute the new values of the dependent variables, and the values computed in the corrector step are not representative of a particular tune so they are denoted with **. The other operators have a similar form.

To retain second-order accuracy overall and not introduce any directional bias; a symmetric application of difference directions is required. Here, the following sequence was used:

Lx1: Predictor, backward difference.

Corrector, forward difference

Ly1: Predictor, backward difference.

Corrector, forward difference

Ly2: Predictor, forward difference.

Corrector, backward difference

LX2: Predictor, forward difference

Corrector, backward difference

Thus, a fractional step Mac Cormack scheme was applied to the overland flow equations, with second-order accuracy in both time and space.

(B) Lateral inflow and interactive infiltration

A goal of this study was to account for fully interactive infiltration when computing lateral inflow rates such that the effects of the relationship between micro topography and infiltration characteristics on run-off could be explored. The occurrence of Horton an overland flow is completely determined by rainfall and ground surface infiltration characteristics Therefore, rainfall was considered constant in time when applied, and a common infiltration model was used; it is the dynamic interaction allowed between surface water and infiltration due to spatial variations in infiltration parameters and micro topogra-

phy that is unique in this model, not the infiltration model itself.

Saturation excess (Dunne) run-off generation is another important hydrologic mechanism related to overland flow, in which the soil surface becomes saturated from below (e.g. due to rising groundwater), thus precluding infiltration.

Currently, every node is considered to be initially not ponded (no surface water, but with the soil at a specified initial moisture content), and the infiltration capacity is greater than the rate of water supplied, the infiltration capacity at every computational node prior to ponding is determined by the well-known Green-Ampt infiltration model.

$$f_{c,j,k} = k_{j,k} \left[\frac{\psi_{j,k} \Delta \theta_{j,k}}{F_{j,k}} + 1 \right],$$

Where K is the effective hydraulic conductivity, ψ is the wetting front suction, θ is the volumetric moisture content deficit (capacity minus initial) at the wetting front, and F is the cumulative depth of water infiltrated. The rate of water available to infiltrate is equal to the rainfall rate, r, plus any flow onto the node from adjacent nodes

$$i_{a,j,k} = r + \frac{q_{x\ on}^n}{\Delta x} + \frac{q_{y\ on}^n}{\Delta y} \dots\dots\dots (21)$$

Where $q_{x\ on}$ and $q_{y\ on}$ are determined by summing the adjacent-node discharges that are in the direction of node (j, k). In this manner, overland flow generated in one area is allowed to infiltrate into other areas if the capacity exists at any time in the simulation; thus, fully interactive infiltration is simulated. If the node remains unponded ($f_c < i_a$), then the average infiltration rate over the time step is determined

$$f_{j,k}^{ave} = i_{a,j,k} \dots\dots\dots (22)$$

Though the time steps normally used in these simulations are very small and the error associated

With not allowing for this phenomenon is likely negligible.

If a node is ponded ($f_c > i_a$), the rate available to infiltrate includes the depth of water on that node

$$i_{a,j,k} = r + \frac{h_{j,k}^n}{\Delta t} + \frac{q_{x\ on}^n}{\Delta x} + \frac{q_{y\ on}^n}{\Delta y} \dots\dots\dots (23)$$

If this rate is greater than the infiltration capacity, $F_{n+1} + I$ is computed using the Green-Ampt equation for cumulative infiltration

$$F_{j,k}^{n+1} - F_{j,k}^n - \psi_{j,k} \ln \left[\frac{F_{j,k}^{n+1} + \psi_{j,k} \Delta \theta_{j,k}}{F_{j,k}^n + \psi_{j,k} \Delta \theta_{j,k}} \right] = k_{j,k} \Delta t, \dots\dots\dots (24)$$

Which is solved using the well-known Newton-Raphson method The average infiltration rate over the time interval is then estimated

$$F_{j,k}^{ave} = \frac{F_{j,k}^{n+1} - F_{j,k}^n}{\Delta t} \dots\dots\dots (25)$$

In both cases, the average lateral inflow rate at a point over the time step is computed as the difference between the rainfall rate and the infiltration rate

$$q_{l,j,k} = r - F_{j,k}^{ave} \dots\dots\dots (26)$$

And is held constant over each time step This source term does not act in the x- or y-direction (q_1 is assumed to be added to the control volume vertically), so half the computed value is applied in the x-direction fractional steps, and half in the y-direction.

As defined here, lateral inflow at any particular node (j, k) can vary from a minimum value equal to

$$q_{lmin} = - \frac{h}{\Delta t} + \frac{q_{x\ on}}{\Delta x} + \frac{q_{y\ on}}{\Delta y} \dots\dots\dots (27)$$

Where all surface water on the node and coming towards the node from adjacent nodes is infiltrated, to a maximum value of

$$q_{lmax} = r, \dots\dots\dots (28)$$

Which is the case for rainfall on an impervious surface Typically, lateral inflow varies from 0 to r in rainfall excess-type hydrologic models, although minimum values equal to $-h/At$ occur in models that allow partial interaction, i.e. only after rainfall

4. RESULTS AND DISCUSSION

Comparative examples

The general properties of the basic Mac Cormack scheme and numerous numerical tests of it related to similar equation sets have been reported elsewhere Here this paper presents the results of several numerical comparisons performed to show the developed models effectiveness related to spatially variable overland flow. four comparisons are made: (1) steady state results are compared with the kinematic wave 'solution' for a plane with "constant lateral inflow, (2) a comparison is made with an analytical solution of a dam break (p756lem7J3) model results are compared with results of an experiment where spatially variable lateral flow was applied to a three-plane cascade, (3) and (4) but flow hydro graphs are computed and compared with some recently published results for overland flow on an infiltrating plane. The first comparative example is used as a general indicator of the ability of the hydrodynamic model to predict the flow variables for a simple case.

Results from rainfall run-off experimental simulations on a 24 m long cascade of three aluminum planes with spatially variable lateral inflow configured such that shocks form are compared with model results in the third example. Each plane section was 8 m long, with slopes of 0.02, 0.015 and 0.01 in the downstream direction. In the most difficult scenario to simulate, each section received constant lateral inflows of 389, 230 and 288 cm h-1 respectively, for a duration of 10 s./Figure.2 shows the model-predicted outflow hydrograph compared with the experimental result produced with .In this experiment, a shock wave is produced, which arrives at the downstream end of the cascade at approximately 25 s; the developed model reproduces these results well considering the potential experimental errors, such as non-uniform lateral inflow, and better than other published analytical and numerical methods. Here, Manning's equation was used to compute friction slope, with a friction coefficient of 0.009.

Table I, Input parameters for the steady state kinematic wave test

Lateral inflow	25.4 mm h-1
Length of plane	30.48 m
Bed slope	0.05
D-W friction factor	0.265

Table II. Results for the steady state kinematic wave test

	Depth (cm)	Discharge (cm2 s-1)
Kinematic wave	0.1462	2.1505
Hydrodynamic model	0.1471	2.1418
Percent difference	0.62	0.40

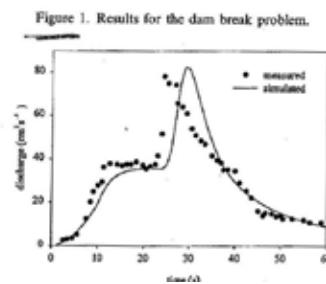


Figure:1 Results for dam break problem

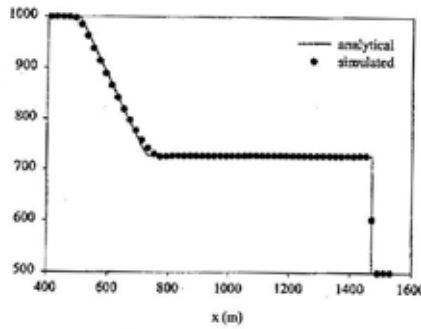


Figure 2. Measured and simulated results for Iwagaki's experiment

The fourth comparison uses some recently published results of overland flow simulations on a 50 m long plane with spatially variable infiltration parameter. Their model is comprised of the kinematic wave equations coupled to the Smith-Parlange infiltration equation solved with a finite difference scheme on a characteristic computational net. There are several important differences between their model and the current model that must be described before the comparison is made.

A different infiltration model was used to compute lateral inflow; however, proper choice of the Green-Ampt parameters *P and A0 corresponding to the Smith-Parlange parameter B will cause the models to yield almost identical results. These near-equivalent parameters are derived using the approximation of Young's for the soil sorptivity, S

And the relationship between the smith-parlange infiltration model parameters B and S

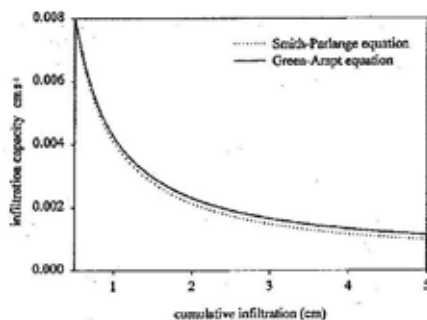


Figure 3. Infiltration capacity curves for the Green- Ampt & Smith-Parlange infiltration capacity Curves with near-equivalent parameters

Were 2.37×10^{-4} and $4.7 \times 10^{-4} \text{ cm s}^{-1}$ respectively. Other Model parameters are presented in Table III.

Fig 4-5-6 represent case -1, 2, and 3 respectively it is seen from these figures that the hydrodynamic model results are

REFERENCES

1. T. Strelkoff, 'One-dimensional equations of open-channel flow', J. Hydraul Div. ASCE, 95, 861-876 (1969). ~ 2. W. Zhang and T.W. Cundy, 'Modeling of two-dimensional overland flow', Water Resour. Res., 25, 2019-2035 (1989). ~ 3. C.B. Vreugdenhil, Numerical Methods for Shallow-Water Flow, Kluwer Academic Publishers, Dordrecht, 1994. ~ 4. D.A. Woolhiser, 'Simulation of unsteady overland flow', in K. Mahmood and V. Yevjevich (eds.), Unsteady Flow in Open Channels, Vol. 2, Water Resources Publications, Fort Collins, CO, 1975, pp. 485-508. ~ 5. R.W. MacCormack, 'The effect of viscosity in hypervelocity impact cratering', AIAA Paper 69-354, Cincinnati, OH, 1969. ~ 6 F.R. Fiedler, 'Hydrodynamic simulation of overland flow with spatially variable infiltration and microtopogra-phy', Ph.D. Dissertation, Colorado State University, 1997 ~ 7. J.S. Antunes do Carmo, F.J. Seabra Santos and A.B. Almeida, 'Numerical solution of the generalized Serre Equations with the MacCormack finite difference scheme', Int. J. Numer. Methods Fluids, 16, 725-738 (1993) ~ 8. P. Garcia-Navarro and J.M. Saviron, 'MacCormack's method for the numerical simulation of one-dimensional discontinuous open channel flow', J. Hydraul. Res., 30, 95-105 (1992) ~ 9. R. Garcia and R.A.Kahawita Numerical solution of the St. Venant equations with the MacCormack finite-difference scheme', Int. J. Numer. Methods Fluids, 6, 259-274 (1986) ~ 10. D.R. Basco, 'Computation of rapidly varied unsteady free surface flow', US Geological Survey, Water Resources Investigations Report 83-4284, 1987. ~ 11. A.W. Jameson, W. Schmidt and E. Turkel, 'Numerical solutions of the Euler equations by finite volume methods using Runge-Kutta time stepping schemes', AIAA Paper SI-1259, 1981. ~ 12 W.H. Green and G.A. Ampt, 'Studies on soil physics Part I the flow of air and water through soils, J. Agric. Sci., 4, 1-24 (1911) ~ 13. V.T. Chow, D.R. Maidment and L.W. Mays, Applied Hydrology, McGraw-Hill, New York, 1988. ~ 22. R.L. Burden and J.D. Faires, Numerical Analysis, PWS_KENT Publishing Company, Boston, MA, 1989. ~ 14. Y. Iwagaki, 'Fundamental studies on the runoff analysis by characteristics', Disaster Prevention Research Institute Bulletin N. W, Kyoto University, Kyoto, Japan, 1955 ~ 15. R.E. Smith and J-Y Parlange, 'A parameter-efficient hydrologic infiltration model', Water Resour. Res. 14, 533-538 (1978) ~ 13.16. D.R. Maidment, Handbook of Hydrology, McGraw-Hill, New York, 1993.

very close to those produced with a characteristic-based kinematic solution on a plane where the kinematic approximation.

Table III. Input parameters for the infiltrating kinematic wave test

Rainfall rate	177.6 mm h ⁻¹
Rainfall duration	20 Min
Length of Place	50 m
Bed slope	0.04
Manning's n	0.1

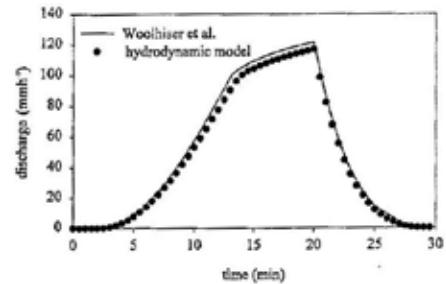


Figure: 4. Results for an infiltrating plane, Uniform k-case (1)

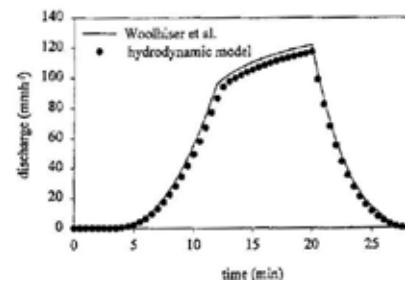


Figure:5 Results for an infiltrating plane, k decreasing down slope - case (2)

F. R. FIEDLER AND J. A. RAMIREZ

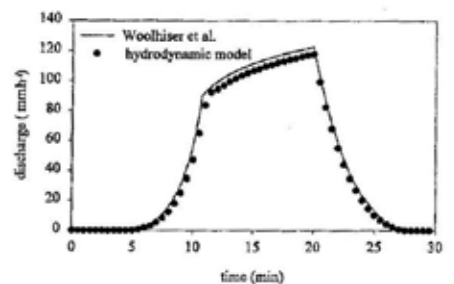


Figure:6 Results for an infiltrating plane, K increasing down slope -case (3)

Should be close to the solution of the full hydrodynamic equations, and the difference is attributable to the different infiltration models.